In situ observation of Ca^{2+} diffusion induced superstructure formation of a rigid polyanion

*Zi Liang Wu[1,†], Riku Takahashi[2], Daisuke Sawada[3], Md. Arifuzzaman[3], Tasuku Nakajima[1], Takayuki Kurokawa[1], Jian Hu[3], and Jian Ping Gong[1,]**

[1]Faculty of Advanced Life Science, Hokkaido University, Sapporo 060-0810, Japan;

[2]Graduate School of Life Science, Hokkaido University, Sapporo 060-0810, Japan;

[3]Graduate School of Science, Hokkaido University, Sapporo 060-0810, Japan.

[†]Present address: Department of Polymer Science and Engineering, Zhejiang University, Hangzhou 310027, China.

*Corresponding author, e-mail: gong@mail.sci.hokudai.ac.jp

Abstract

Diffusion of multivalent metallic ions into aqueous solution of rigid, negatively charged macromolecules of high concentration is an effective approach to prepare macroscopically anisotropic hydrogels. However, the mechanism for superstructure formation is still not clear. By observing the mixing process of a small drop of $CaCl_2$ solution with solution of a rigid polyanion, poly(2,2'-disulfonyl-4,4'-benzidine terephthalamide) (PBDT), under the polarizing optical microscope, the diffusion profile of Ca^{2+} and detailed anisotropic gelation process of PBDT are revealed. Diffusion of Ca^{2+} into the surrounding PBDT solution immediately induces the formation of physical liquid crystalline (LC) gel with concentric alignment of PBDT. The thickness d of this region increases with diffusion time t, obeying the diffusion law $d \sim t^{1/2}$. A thin ring of constant width (~100 μm) with radial alignment of PBDT appears at the diffusion/reaction front, ahead of the concentric alignment region. When two drops of $CaCl_2$ fluxes meet, their outside thin rings interact with each other and the PBDT in this contacting region orients $\pm 45^{o}$ to the midline of the two drops. From these observations, we rationally contend that the internal stress induced by the contraction of gel phase is responsible for the ion diffusion-induced PBDT orientations. This structure formation mechanism gives insight into other diffusion-directed anisotropic gelation systems.

1. Introduction

Hydrogels, a class of soft and wet material, have attracted increasing attentions due to their similarity to soft biotissues, excellent responses to external stimuli, and promising applications in drug delivery systems, tissue engineering, soft actuators, etc.[1] However, the conventional hydrogels are amorphous with isotropic matrix, resulting in absence of many functions such as anisotropic optical or mechanical properties. In contrast, soft biotissues usually possess well-ordered structures of biomacromolecules, endowing the living organisms with excellent functionalities.[2] Many efforts have been made towards developing ordered structures at different scales in hydrogels prior to or during the gelation process, such as by molecular self-assembly, self-segregation, phase separation, and by applying electric or magnetic fields.[3] These ordered structures render hydrogels with versatile additional functionalities.[3b,3f]

Reaction-diffusion (RD) process is another facile approach to develop physical hydrogels with controllable ordered structure, especially in macroscopic scale.[4] In RD process, diffusion and reaction compete and lead to formation of intricate periodic structures. Classic examples are the formation of periodic precipitation or minerals when two solutions with different solutes diffuse and react in a gel matrix.[4a] In recent years, RD process has been applied to develop macroscopically anisotropic liquid crystalline (LC) hydrogels.[5,6] Dobashi et al. have found that the diffusion of multivalent metallic ions induces biomacromolecules such as DNA and curldan to form physical hydrogels with ordered structure. Later, we also found that diffusion of Ca^{2+} ions into aqueous solution of negatively charged rigid polyanion, poly(2,2'-disulfonyl-4,4'-benzidine terephthalamide) (PBDT), leads to the formation of a physical hydrogel with orientation of PBDT perpendicular to the diffusion direction of Ca^{2+}.

Furthermore, a very thin layer that showed opposite orientation to the anisotropic gel appeared at the diffusion front.[6b] However, the structure formation mechanism has not been fully revealed. Yokoyama et al. have prepared an anisotropic alginate hydrogel by extruding sodium alginate aqueous solution from a tube to a solution containing multivalent metallic ions.[7] They found alginate molecules aligned perpendicular to the total flow direction, which was ascribed to diametric expansion and longitudinal shrinkage of the gel.

To reveal this specific structure formation mechanism, an *in situ* observation of the ordered structure formation is indispensable. In this paper, we present a simple method to observe *in situ* the anisotropic gelation during the RD process within a short time and space frame and to reveal the structure formation mechanism of rigid polyanions. A small drop of $CaCl_2$ solution is dripped to a PBDT solution film placed on a slide glass. The radial diffusion of Ca^{2+} into the surrounding region induces PBDT orientation and gelation. Owing to the small size of samples, PBDT orientations could be clearly identified from the birefringence by *in situ* observation under a polarizing optical microscope with a 530 nm tint plate. In addition, scanning electronic microscopy (SEM) with energy dispersive spectroscopy is applied to observe the "frozen" diffusion features and molecular distribution of a dry sample, which is prepared by quickly evaporating all the solvent. The results suggest that the syneresis contraction of the gel phase, which induces the internal stress at the sol-gel interface (the flux front of Ca^{2+}), is responsible for the PBDT orientations.

Previous studies require long time to form bulk anisotropic hydrogels and thus it is massive work to systematically study the effect of various parameters, such as ion concentration and polymer concentration, on the structure formation.[5,6,8] The simple method presented here greatly simplifies the RD experiment and makes the study of diffusion profile

more efficient. Another advantage of this method is that it permits us timely 'freezing' the structure by quickly evaporating all the solvent via heating, when one surface of the system is open to air. The method described in this work is applicable to other diffusion directed gelation process, such as diffusion of acidic/basic agents induced gelation of small molecules or macromolecules.[5,7,9]

2. Experimental Section

Materials

PBDT, a water soluble rigid polyanion, was synthesized by an interfacial polycondensation reaction.[10] The synthesized PBDT has a weight-average molecular weight, M_w, of 2.1×10^6 g/mol; its aqueous solutions have a crossover concentration, C^*, of ~0.2 wt% and a critical low concentration of nematic phase, C_{LC}^*, of 2 wt%.[6b,11] Calcium chloride, palladium chloride, ferric chloride, and sodium chloride (Wako Pure Chemical Industries, Ltd.) were used as purchased. Milli-Q (18.2MΩ cm) water was used in all experiments.

In situ observation of PBDT superstructure formation during the diffusion process

A drop (25 μL) of PBDT solution with prescribed polymer concentrations, C_P, was dripped by a syringe onto a slide glass at ~20 ^oC; the solution spread to a thin film with diameter and thickness of about 1.5 cm and 150 μm, respectively. Subsequently, a drop (5 μL) of $CaCl_2$, $BaCl_2$, or $FeCl_3$ solution with a prescribed concentration was dripped on the central part of the PBDT solution film (Figure 1a). The bottom of $CaCl_2$ drop immediately became turbid once it contacted with the PBDT solution, indicating that some Ca^{2+} ions formed

complex with PBDTs. As other free Ca^{2+} ions diffused into the surrounding PBDT solution and formed complex with PBDTs, the turbid area gradually increased. The whole process was observed *in situ* under polarizing optical microscope (POM; Nikon, LV100POL) with crossed polarizers. A 530 nm sensitive tint plate was inserted to identify the orientations of PBDT.[6b,12] Photo images were taken every 10 s for 10 min until the diffusion flux front reached the edge of the microscope view. Images were also arranged into movies using video editing software.

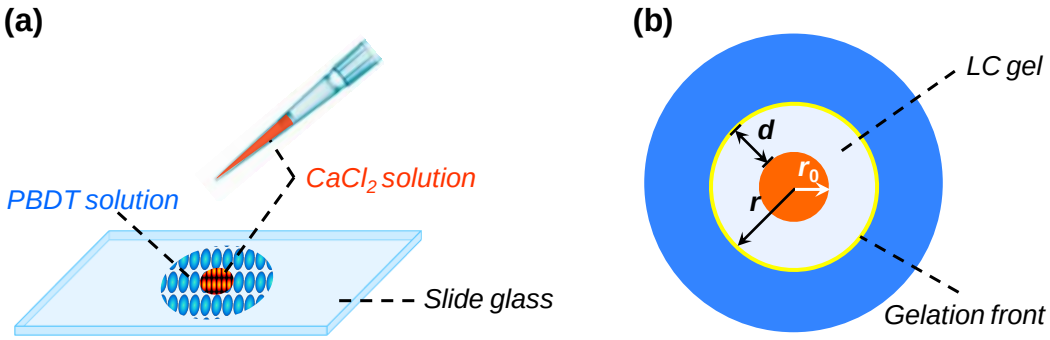

Figure 1. (a) Schematic for the experimental diffusion of Ca^{2+} into PBDT solution. After one drop of $CaCl_2$ solution is dripped onto the central part of PBDT solution, the diffusion of Ca^{2+} induces the surrounding PBDT molecules orientation and gelation to form an anisotropic physical gel. (b) Top view of the diffusion system. r_0, r, and d denote the radius of $CaCl_2$ drop, radius of liquid crystalline (LC) gel, and the width of LC gel, respectively.

Superstructure formation of PBDT at the region between multiple drops of $CaCl_2$ solution was also investigated. Two or three drops of 0.5 M $CaCl_2$ solution were simultaneously dripped to 3 wt% PBDT solution film. Then, the middle region of the sample where two or three Ca^{2+} fluxes met was observed under POM. Images were taken at different diffusion time. Experiments with $BaCl_2$ and $FeCl_3$ instead of $CaCl_2$ were performed in a similar process.

Scanning electronic microscopy (SEM) observation of the gel

SEM with energy dispersive spectroscopy (JSM-6010LA, JEOL Ltd.) was applied to study the morphology and element distribution of the dry sample. The wet sample on a cover glass after 3 min diffusion was transferred to a hot plate (temperature: 90 ^{o}C) to rapidly evaporate the solvent within ~20 s and freeze the molecular distribution. The dry sample coated with a thin Au by using a sputter coater (E-1030, Hitachi) was used for SEM observation and X-ray element mapping of sulfur and calcium. The intensity profile of element was obtained from the mapping image by using Image J.

3. Results and Discussion

3.1 *In situ* observation of reaction-diffusion profile

First of all, we should note that the present system has two features, as summarized in Table 1: (i) PBDT chains were entangled to give highly viscosity of the polymer solution, as the polymer concentration was well above its overlap concentration ($C_P/C^* >> 1$);[11a] (ii) locally, the concentration of Ca^{2+} is comparable to or in excess of the concentration of the sulfonic charge of PBDT, $C_{p,charge}$. Owing to the relatively small size of samples, we can directly observe *in situ* the reaction-diffusion (RD) process under POM. The PBDT solution with C_P = 1 wt% (< C_{LC}* of 2 wt%) was optically isotropic. However, a birefringence ring, with alternative blue (quadrants 2 and 4) and orange (quadrants 1 and 3) colors, appeared immediately when a drop of 0.5 M Ca^{2+} was dripped on the PBDT solution (Figure 2a). The ring size gradually grew with time, increasing its outer radius *r* and thickness *d,* while the inner radius of the ring r_0 hardly changed. However, the intensity of the birefringence slightly decreased with the diffusion distance, indicating a decrease in the extent of molecular

alignment. At the boundary, i.e. the gelation front,[13,14] there was a thin ring with birefringence color opposite to that of the LC gel. As PBDT is an optically positive polymer,[6b,12] the PBDT molecules in the birefringence ring can be identified as in concentric orientation, while those in the thin ring at the diffusion front are in radial orientation. After 10 min diffusion, the birefringence ring was close to the edge of POM image.[15] The growth of these birefringence patterns is associated to the diffusion of Ca^{2+} ions into surrounding PBDT solution, leading to the formation of anisotropic liquid crystalline (LC) hydrogel, which was not dissolvable after being immersed in water.

Table 1. Apparent diffusion coefficient, D, of Ca^{2+} in the diffusion systems with different C_P and C_{Ca2+} at 20 °C.[a]

PBDT concentration			$C_{Ca^{2+}}$ (M)			
C_P (wt%)	C_P/C^* [b]	$C_{p,charge}$ (M) [c]	0.1	0.5	1	2
1	5	0.04	9.8×10^{-6} (0.62)	2.6×10^{-5} (1.64)	3.2×10^{-5} (2.02)	3.4×10^{-5} (2.15)
2	10	0.08	6.3×10^{-6} (0.40)	2.0×10^{-5} (1.26)	2.7×10^{-5} (1.71)	2.8×10^{-5} (1.77)
3	15	0.12	3.0×10^{-6} (0.19)	1.6×10^{-5} (1.01)	2.4×10^{-5} (1.52)	2.6×10^{-5} (1.64)

[a] The values of D with unit of $cm^2 \cdot s^{-1}$ calculated according to $d^2 = 2Dt$ are listed in the shadow part of the table. The values in brackets are D/D_0, in which D_0 of Ca^{2+} in pure water at 20 °C is 1.58×10^{-5} $cm^2 \cdot s^{-1}$. [b] Corresponding ratio of C_P to crossover concentration of PBDT, C^*, of 0.2 wt%. [c] Corresponding molar concentration of the charge ($C_{p,charge}$), in which each repeat unit of PBDT has two charged sulfonic groups.

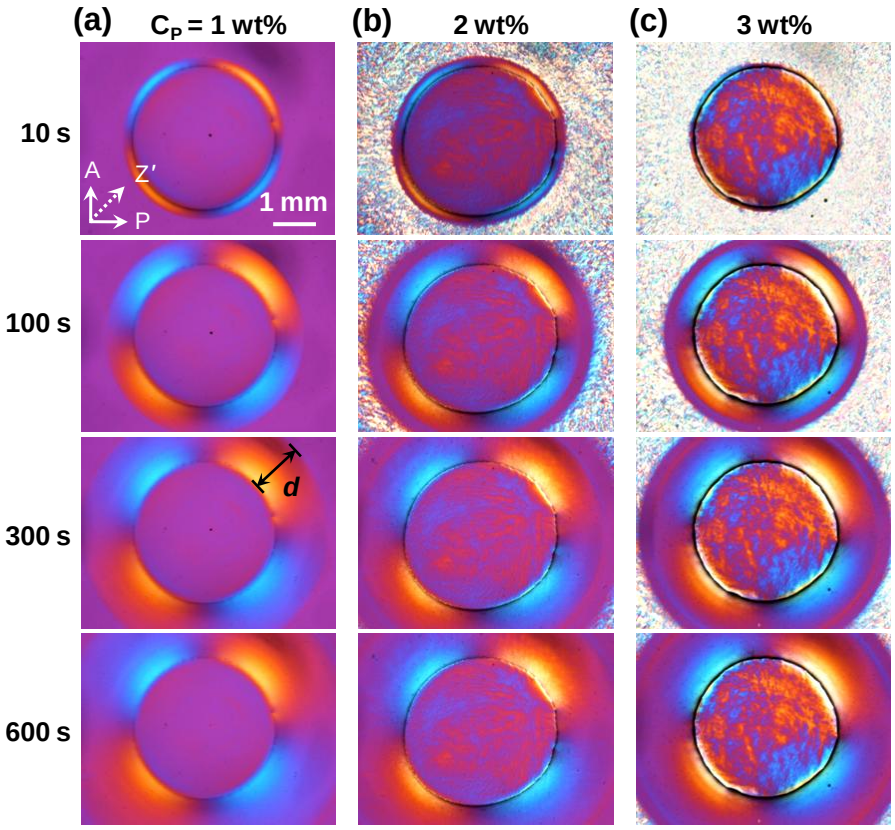

Figure 2. Images to show diffusion-induced formation of LC gel observed *in situ* at different diffusion time under polarizing optical microscope (POM) with 530 nm tint plate. C_{Ca2+} = 0.5 M, C_P = 1 wt% (a), 2 wt% (b), and 3 wt% (c). The *d* noted in the third image of the left column is the width of LC gel. A: Analyzer; P: Polarizer; Z′: Slow axis of the tint plate.

This facile method with accessible, accurate diffusion time and distance from POM images permits us quantitatively studying the diffusion features under different experimental conditions. We found that the systems at (C_P = 2 wt%) or above (C_P = 3wt%) C_{LC}* of PBDT showed similar birefringence pattern evolution with diffusion time (Figure 2b and 2c; Movies S1-S3 in Supporting Information). Furthermore, similar phenomena were also observed in the systems with other Ca^{2+} concentrations (C_{Ca2+} = 0.1, 1, 2 M).

The gelation and the molecular orientation of PBDT are related to the diffusion of Ca^{2+}. This is confirmed by the linear relationship observed between the LC gel thickness square d^2

and the diffusion time t, as shown in Figure 3a and Figure S1 (see Supporting Information). According to $d^2 = 2Dt$,[16] the slope of the linear lines gives the apparent diffusion coefficient D, which is listed in Table 1. D obtained here for C_{Ca2+} = 0.5 M, C_P = 1 and 2 wt% systems was 2 $\times 10^{-5}$ and 2.6 $\times 10^{-5}$ $cm^2 \cdot s^{-1}$, respectively, which were close to 2.4 $\times 10^{-5}$ $cm^2 \cdot s^{-1}$ obtained by long time diffusion,[6b] indicating good reliability of this facial method. D increased as C_{Ca2+} increased, yet it decreased as C_P increased (Table 1). When C_{Ca2+} = 0.1 M, the apparent D was smaller than the diffusion coefficient D_0 of Ca^{2+} in pure water ($D/D_0 < 1$; $D_0 = 1.58 \times 10^{-5}$ $cm^2 \cdot s^{-1}$, at 20 °C).[5c,17] On the other hand, when C_{Ca2+} = 0.5, 1, 2 M, $D/D_0 > 1$.

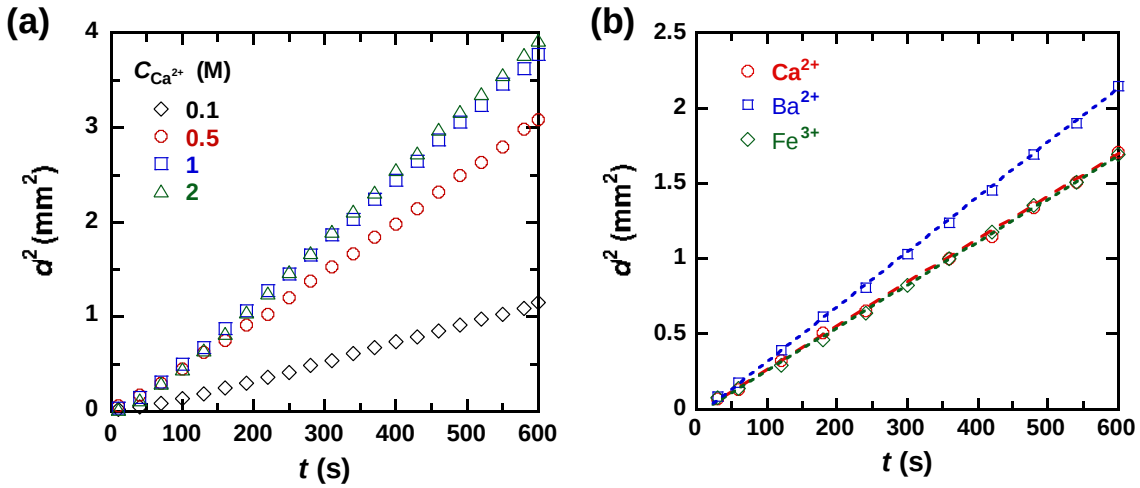

Figure 3. Relationship of square of LC gel width, d^2, versus diffusion time, t. (a) Systems with C_P = 1 wt% and different C_{Ca2+}, (b) systems with C_P = 3 wt% and 0.5 M of $CaCl_2$, $BaCl_2$, or $FeCl_3$.

Due to the high viscosity of PBDT solution, the translational motion of PBDT macromolecules can be neglected in comparison with that of small Ca^{2+} ions. So the gelation was essentially a Ca^{2+} diffusion-limited reaction.[8a] The diffusion of Ca^{2+} was affected by the reaction, i.e. the complexation between PBDT and Ca^{2+}, in terms of two aspects. (i) The reaction, including complexation and gelation of PBDTs, immobilizes Ca^{2+} and decreases the

amount of local free Ca^{2+}, forming a sharp concentration gradient of mobile Ca^{2+} at the diffusion front. According to Fick's first law, the diffusion flux is proportional to the negative of the concentration gradient. Therefore, the complexation, which builds up a sharp concentration gradient at the diffusion front, should promote the diffusion process. (ii) The reaction front continuously consumes the free Ca^{2+} just diffused through previously formed gel matrix, which hinders to some extent the diffusion of Ca^{2+} over the reaction front. This effect becomes evident especially when the fresh flux of Ca^{2+} can not gelate all the PBDTs at once. The above two effects competed with each other and determined the apparent value of D listed in Table 1. When $C_{Ca2+} = 0.1$ M, the effect (ii) predominated, resulting in the apparent D smaller than D_0 of Ca^{2+} in pure water ($D/D_0 < 1$). For example, when $C_P = 3$ wt%, D/D_0 was only 0.19. When $C_{Ca2+} \geq 0.5$ M, the effect (i) predominated, and $D/D_0 > 1$. C_P affected the apparent D in another way: increase in C_P consumes more Ca^{2+} for complexation, which would enhance the above effect (ii) of C_{Ca2+}. In addition, high C_P means less free volume and a more restricted medium, which hinders to some extent the diffusion of Ca^{2+} through the gel matrix to the reaction front. Therefore, increase in C_P decreased the apparent D, as shown in Table 1.

This facile approach also permits us comparing the effects of different metallic ions on the diffusion-directed anisotropic gelation of PBDT solutions by keeping the concentration of PBDT and metallic ions constant, 3 wt% and 0.5 M, respectively. According to the different slopes of d^2 versus t (Figure 3b), we can see that Fe^{3+} and Ca^{2+} have a similar apparent D (1.5×10^{-5} $cm^2 \cdot s^{-1}$), which is smaller than that of Ba^{2+} (1.9×10^{-5} $cm^2 \cdot s^{-1}$).

3.2 Complex superstructures formed during the diffusion

To reveal the structure formation mechanism, the birefringence patterns were analyzed in detail. As shown in Figure 4a, in the system with C_P = 1 wt% and C_{Ca2+} = 0.5 M, the ring with strong birefringence appeared right after the diffusion started and grew in thickness as the diffusion proceeded (Figure 4a). PBDT molecules in the birefringence ring can be identified as in concentric orientation. However, a thin ring with radial alignment of PBDTs, in vertical to PBDT in the LC gel appeared at the diffusion/reaction front after a short diffusion time, t ~ 80 s. This thin ring kept a constant ring thickness of ~100 μm, moved forward and became clearer as the diffusion continued.

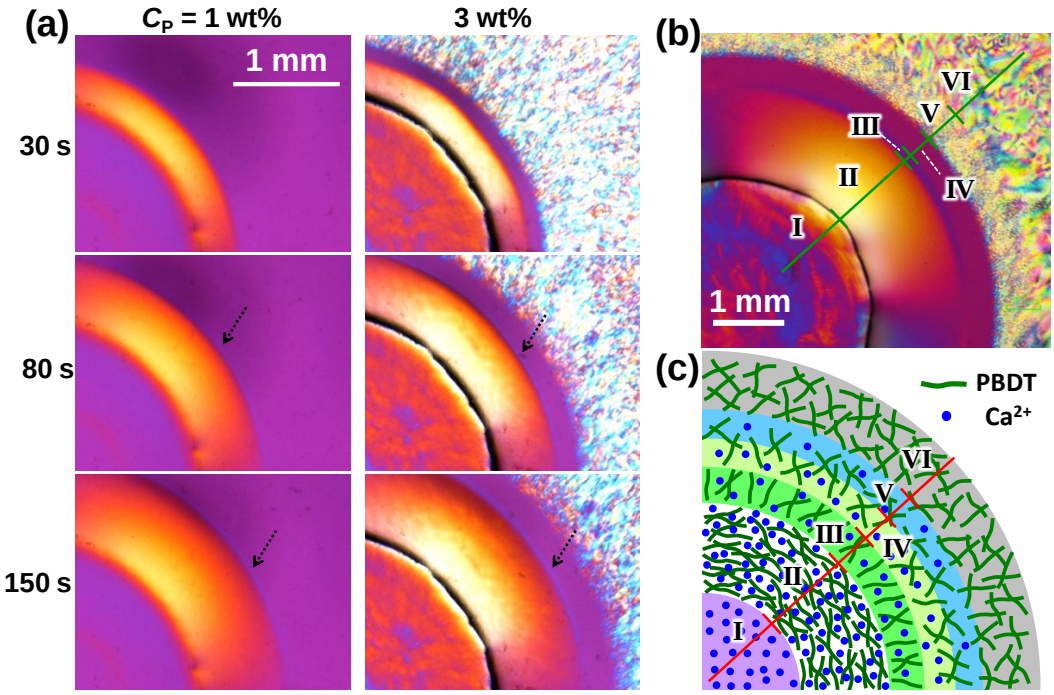

Figure 4. (a) POM images to show Ca^{2+} diffusion-induced superstructure formation of PBDT; C_{Ca2+} = 0.5 M, C_P = 1 wt% (left column) and C_P = 3 wt% (right column). Only quarters of the ring images are shown to save the space. Arrows show the existence of a thin ring with birefringence color opposite to that of LC gel. (b) POM image of the system with different localized states of PBDT after 10 min diffusion of Ca^{2+}; C_P = 3 wt%, C_{Ca2+} = 0.5 M. Regions I to VI correspond to the Ca^{2+} drop, LC gel with concentric alignment of PBDT, thin ring with radial alignment of PBDT, isotropic region, N-I transition region, and nematic phase of PBDT solution, respectively. (c) Schematic for the corresponding PBDT alignments in the reaction-

diffusion process (right upper quadrant). The layer thicknesses in the illustration are not in scale; the counter ions Na^+ and Cl^- of PBDT and Ca^{2+}, respectively, are omitted for simplicity.

In the case of C_P = 3 wt% (> C_{LC}* of 2 wt%), the thick birefringence ring with concentric alignment of PBDT also appeared (region II; Figure 4b and 4c), which is the same as the case of C_P = 1 wt%. When the diffusion started (t = 30 s), a new narrow purple ring (region IV), corresponding to an isotropic phase, appeared between the birefringence ring and LC texture of PBDT solution. Near the amorphous ring, a ring with disturbed LC structure (region V) from the original Schlieren texture (region VI) of the nematic PBDT solution was also observed (Figure 4b). When t > 80 s, the narrow ring with radial alignment of PBDT (region III) also appeared between the thick birefringent ring (region II) and the isotropic purple ring (region IV). The width of isotropic ring became larger as the diffusion proceeded (it was ~0.5 mm at t = 10 min). These results indicate an identical mechanism for the structure formation, no matter C_P is above or below C_{LC}*. The above phenomena and features observed within a short time and space frame are identical to those observed during the formation of bulk anisotropic gels.[6b]

The nematic to isotropic (N-I) phase transition of PBDT in regions IV and V might originate from (i) the decrease in local C_P from 3 wt% to C_P lower than C_{LC}* of 2 wt%, or (ii) the disordered structure of molecular assemblies by the interaction of PBDTs with a small amount of metallic ions. To verify these speculations, the morphology of dry sample after fast solvent evaporation and the "frozen" distributions of PBDT and calcium were studied by SEM with energy dispersive spectroscopy (Figure 5). In the dry sample, the isotropic ring region also showed birefringence (Figure 5b); however, the thin ring with radial orientation of

PBDTs in wet sample could not be identified. We considered that the thin ring region and isotropic region (regions III and IV, respectively, in Figure 5a), corresponding to the weak physical gel, combined to form an integrated region (i.e. region iii+iv in Figure 5b) after drying. SEM observation also showed clear boundaries of these regions, indicating their different structures (Figure 5c). From the element distribution profile, we have not observed an abrupt decrease in PBDT content at the isotropic region (Figure 5d), indicating that the N-I transition was not due to the decrease in C_P. On the other hand, calcium appeared in the isotropic region and in the N-I transition region (Figure 5e; corresponding to region iii+iv and region v in Figure 5b), although the local C_{Ca2+} was lower than that in the LC gel (Figure 5f). This result suggests that a small amount of Ca^{2+} might induce the N-I transition of PBDT.

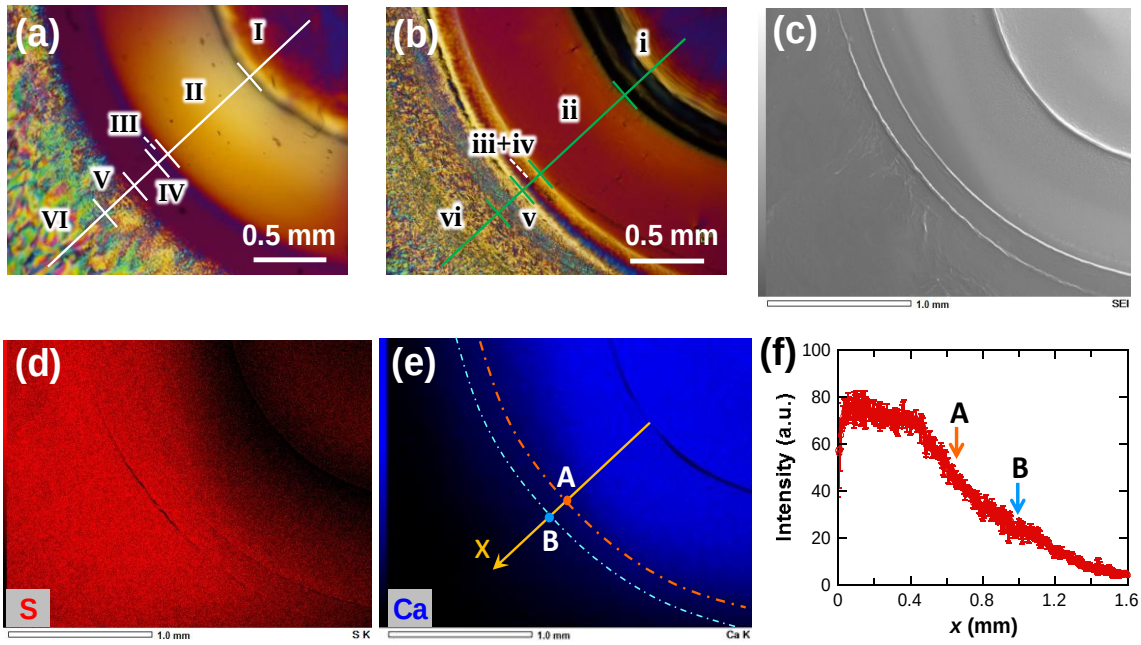

Figure 5. (a, b) POM images of the sample used for SEM observation; (a) wet sample, C_P = 3 wt%, C_{Ca2+} = 0.5 M, t = 2 min, (b) dry sample, all the solvents were quickly evaporated upon heating. Regions I to VI in Figure 5a are divided as those in Figure 4b; regions i to vi in Figure 5b after solvent evaporation correspond to regions I to VI in Figure 5a. (c-e) SEM images of the dry sample (c) and its element distributions of sulfur (d) and calcium (e). (f) Intensity profile of image (e) in the radius direction.

To confirm further the above assumption that a small amount of Ca^{2+} ions can induce N-I transition of PBDT, a drop of $CaCl_2$ solution with C_{Ca2+} of 0.05 M, instead of that with C_{Ca2+} of 0.5 M used in the above observations, was dripped onto 3 wt% PBDT solution. We found no anisotropic LC gel formed. Yet the PBDT solution in the nematic phase changed to isotropic phase when Ca^{2+} diffused in (Figure S2). This effect of Ca^{2+} induced N-I transition is similar to that of Na^+.[11a] Low concentration of metallic ions can disturb the subtle balance of intermolecular interactions and induce conformational collapse of charged rigid polyelectrolytes.[18] We therefore conclude that the appearance of isotropic phase and N-I transition of PBDT (corresponding to regions IV and V in Figure 4b) during the diffusion process is due to the interaction between PBDTs and a small amount of Ca^{2+} ions, which disturbs to some extent the assembled structure of PBDTs. As C_{Ca2+} gradually increased, above 0.1 M, PBDT/Ca^{2+} complexes formed an integrated strong anisotropic LC gel, changing from an isotropic liquid or weak physical gel.

3.3 Proposed mechanism for superstructure formation

To reveal the essential mechanism for the structure formation of PBDT during the RD process, especially the radial alignment of PBDT in the thin ring region at the reaction/diffusion front, we dripped simultaneously two drops of 0.5 M $CaCl_2$ solution to 3 wt% PBDT solution and observed the superstructure formation at the middle region where two fluxes of Ca^{2+} met after a period of diffusion time. Before the two fluxes met, the molecular orientation is identical to that of the diffusion system with one drop of Ca^{2+} (Figure 6a(i)-(iii)). However, as the diffusion proceeded, the width of LC gels grew, so the two thin birefringence rings with radial alignment of PBDTs in the diffusion fronts started to meet (Figure 6a(iv)).

At the contacting region, the birefringence became much stronger. When the LC gels grew further, the new formed contacting region also showed strong birefringence (Movie S4). As a result, a strong and long birefringence pattern with alternative colors, which are opposite to those of neighboring LC gels, appeared between the two LC gels. When we rotated the sample 45^{o}, the previous strong birefringence pattern almost disappeared (Figure 6b, Figure S3, and Movie S5), indicating that at the contacting region PBDTs oriented $\pm$45^{o} to the midline of the two drops (Figure 7b), which is different from the radial alignment before two thin rings met (Figure 7a). This region with special alignment of PBDTs and birefringence much stronger than other part of the thin ring could not be explained by molecular migration proposed in our previous paper.[6b] In our recent work, we found that PBDT molecules are easy to be aligned by a small external strain (ε ~5%) or internal stress, which generate strong birefringence.[19,20] This internal stress induced PBDT orientation should also exist in the current RD process, leading to the formation of different alignments of PBDTs.

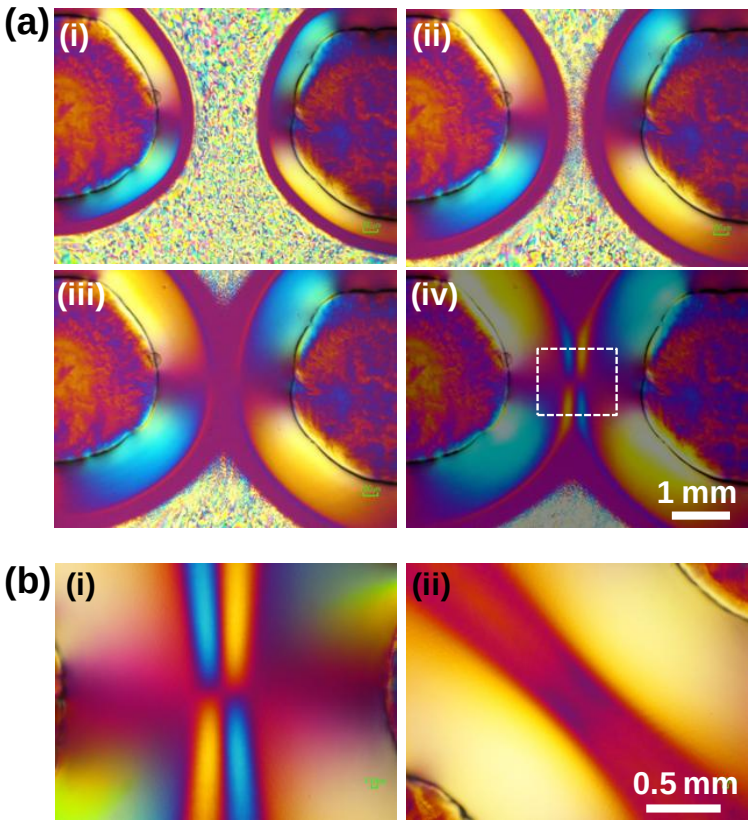

Figure 6. (a) POM images of the systems with two drops of Ca^{2+} dripped into PBDT solution at different diffusion time, *t*. C_P = 3 wt%, C_{Ca2+} = 0.5 M; (i) *t* = 1 min, (ii) *t* = 2 min, (iii) *t* = 4 min, and (iv) *t* = 6 min. (b) POM images of the contacting zone of the two LC gels (i) and after 45^o rotation counter clockwise (ii).

As the Ca^{2+} diffused into the surrounding PBDT solution, a weak physical gel formed at the diffusion front where C_{Ca2+} is very low.[14] However, as more Ca^{2+} diffused in with local C_{Ca2+} above a critical value, more ion complexation is formed and the physical gel became strong. During this process, contraction of gel volume occurs due to decreased osmotic pressure of the PBDT solution by complexation.[21] The contraction of the strong gel phase results in the concentric alignment of PBDTs in the gel; it also leads to the radial alignment of PBDTs in front of the strong gel, where weak physical gel is forming (Figure 7a; PBDTs align along the tensile force). This scenario repeated at the diffusion front, changing on site the

superstructure of PBDTs from radial alignment to concentric alignment, when the weak physical gel became strong one. The region of weak gel with radial alignment of PBDTs is very thin, ~100 μm, probably because the stress is dissipated easily in the new formed weak gel (i.e. region IV in Figure 4b). When two Ca^{2+} fluxes from two drops meet at the middle position, the local weak gel is stretched from two directions by the contraction of two strong LC gels, leading to the birefringence much stronger than other part of the thin ring. As more Ca^{2+} ions diffuse to this contacting region, the localized physical gel becomes stronger and contracts due to the syneresis effect. Therefore, another stretching force along the contacting line and toward the center of the middle gel appears. Under these two kinds of forces, PBDTs in the new formed weak physical gel region orient approximate $\pm 45^{o}$ to midline of the two drops (Figure 7b).

The same phenomena appeared in the system with three drops of Ca^{2+}. After a certain diffusion time, the center became a relatively closed region without severely molecular migration, yet strong birefringence appeared with colors different from those of neighbouring preformed LC gels (Figure S4). This result further supported the mechanism we proposed in Figure 7.

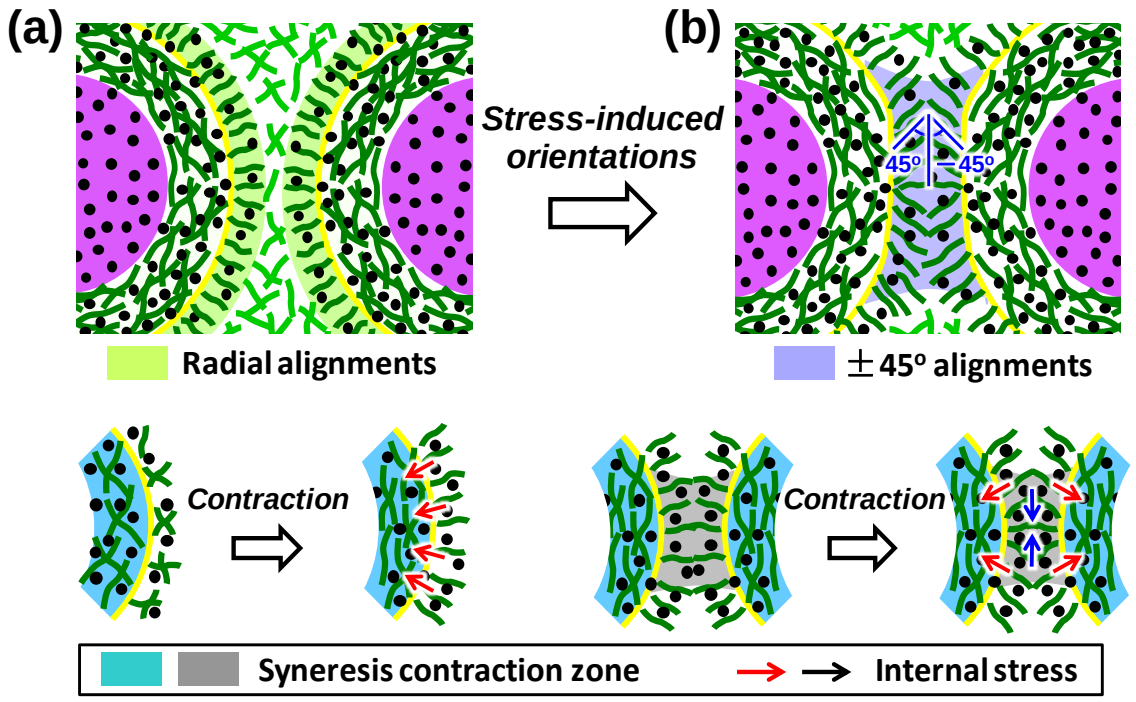

Figure 7. Schematic for the PBDT alignments in the reaction-diffusion process and the corresponding mechanism for PBDT orientations in the diffusion system with two drops of Ca^{2+} solution. (a) During the complexation between PBDT and Ca^{2+}, physical LC gel forms, accompanying with syneresis contraction of the gel volume, which builds internal stress and induces PBDT alignments. As a result, PBDTs in the heavily gelated part under the compression form concentric alignments, whereas PBDTs in the outer weak physical gel part under the tension (the weak gel is stretched by the contraction of LC gel) form radial alignments. (b) When the two fluxes of Ca^{2+} meet at the intermediate section, the new formed weak physical gel is stretched by two forces from the syneresis contractions of LC gel and the central weak gel (which becomes stronger after PBDTs complex with more Ca^{2+} ions). Therefore, the internal stresses induce PBDTs in new formed weak gel at the intermediate region to orient $\pm 45^{o}$ to the boundary (midline) where two Ca^{2+} fluxes meet.

In Figure 4a, we found that the formation of a thin ring with radial alignment of PBDT is not immediate but after a short diffusion time, t ~ 80 s. This is likely because the physical gelation and syneresis contraction of gel do not complete immediately when PBDT meets Ca^{2+} but take some time.[21] We contend here the contraction of the gel and the stress induced PBDT orientation as the essential reasons for the structure formation of the gel. When Ca^{2+} is

changed to Ba^{2+} or Fe^{3+}, we observed the same phenomena described above, indicating the universality of the mechanism, which gives insight to develop other hydrogels from rigid biomacromolecules and multivalent metallic ions based on the RD process.

4. Conclusions

In this paper, we have presented a simple method to study the Ca^{2+} diffusion-directed anisotropic gelation of a rigid polyanion, PBDT, and revealed the mechanism for ordered structure formation. By dripping a small drop of Ca^{2+} solution on a thin film of PBDT solution, the diffusion-induced structure formation and gelation process could be observed *in situ* under POM within a short time and space frame, permitting us effectively studying the structure formation under various experimental conditions. The diffusion features and the molecular orientations within this small system are consistent well with the formation of bulk gels.[6b] The diffusion of Ca^{2+} produces a physical LC hydrogel with concentric alignment of PBDTs, owing to the syneresis contraction of the physical gel in the radial direction. In front of the LC gel phase (i.e. at the diffusion/reaction front), a ~100 μm width ring with radial orientation of PBDTs, in perpendicular to those of the LC gel phase, always exists except at the initial ~80 s diffusion. This thin ring with radial alignment of PBDT is the result of the mechanical interaction between the strong LC gel that intends to contract and the weak gel that is stretched by the contraction. This work provides a simple way to study the RD process and reveals the structure formation mechanism of ion complex formation of rigid molecules, which should be suitable to other systems.

Acknowledgments

This research was financially supported by a Grant-in-Aid for Scientific Research (S) (No. 124225006) from Japan Society for the Promotion of Science (JSPS).

Supporting Information Available: POM images of the samples observed with and without 530 nm tint plate; movies to show the birefringence change during the diffusion process of two PBDT drops and rotation of the sample.

References

(1) (a) Osada, Y.; Gong, J. P. *Adv. Mater.* **1998**, *10*, 827. (b) Lee, K. Y.; Mooney, D. J. *Chem. Rev.* **2001**, *101*, 1869. (c) Calvert, P. *Adv. Mater.* **2009**, *21*, 743. (d) Slaughter, B. V.; Khurshid, S. S.; Fisher, O. Z.; Khademhosseini, A.; Peppas, N. A. *Adv. Mater.* **2009**, *21*, 3307. (e) Qiu, Y.; Park, K. *Adv. Drug Deliv. Rev.* **2001**, *53*, 321. (f) Keplinger, C.; Sun, J.-Y.; Foo, C. C.; Rothemund, P.; Whitesides, G. M.; Suo, Z. *Science* **2013**, *341*, 984.

(2) (a) Sanchez, C.; Arribart, H.; Giraud-Guille, M. M. *Nat. Mater.* **2005**, *4*, 277. (b) Gartner, L. P.; Hiatt, J. L. *Color Textbook of Histology, 2nd ed*., Saunders: Philadelphia, **2001**.

(3) (a) Kato, T. *Science* **2002**, *295*, 2414. (b) Kang, K.; Walish, J. J.; Gorishnyy, T.; Thomas, E. L. *Nat. Mater.* **2007**, *6*, 957. (c) Zhang, S. M.; Greenfield, M. A.; Mata, A.; Palmer, L. C.; Bitton, R.; Mantei, J. R.; Aparicio, C.; de la Cruz, M. O.; Stupp, S. I. *Nat. Mater.* **2010**, *9*, 594. (d) Harada, A.; Kobayashi, R.; Takashima, Y.; Hashidzume, A.; Yamaguchi, H. *Nat. Chem.* **2011**, *3*, 34. (e) Gao, Y.; Zhao, F.; Wang, Q.; Zhang, Y.; Xu, B. *Chem. Soc. Rev.* **2010**, *39*, 3425. (f) Wu, Z. L.; Gong, J. P. *NPG Asia Mater.* **2011**, *3*, 57. (g) Haque, M. A.; Kamita, G.; Kurokawa, T.; Tsujii, K.; Gong, J. P. *Adv. Mater.* **2010**, *22*, 5110. (h) Haque, M. A.; Kurokawa, T.; Kamita, G.; Gong, J. P. *Macromolecules* **2011**, *44*, 8916. (i) Yan, X. Z.; Wang, F.; Zheng, B.; Huang, F. H. *Chem. Soc. Rev.* **2012**, *41*, 6042.

(4) (a) Liesegang, R. E. *Naturwiss. Wochenschr.* **1896**, *11*, 353. (b) Grzybowski, B. A.; Bishop, K. J. M.; Campbell, C. J.; Fialkowski, M.; Smoukov, S. K. *Soft Matter* **2005**, *1*, 114. (c) Grzybowski, B. A.; Campbell, C. J. *Mater. Today* **2007**, *10*, 38. (d) Capito, R. M.; Azevedo, H. S.; Velichko, Y. S.; Mata, A.; Stupp, S. I. *Science* **2008**, *319*, 1812.

(5) (a) Dobashi, T.; Nobe, M.; Yoshihara, H.; Konno, A. *Langmuir* **2004**, *20*, 6530. (b)

Dobashi, T.; Furusawa, K.; Kita, E.; Minamisawa, Y.; Yamamoto, T. *Langmuir* **2007**, *23*, 1303. (c) Nobe, M.; Dobashi, T.; Yamamoto, T. *Langmuir* **2005**, *21*, 8155. (d) Furusawa, K.; Minamisawa, Y.; Dobashi, T.; Yamamoto, T. *J. Phys. Chem. B* **2007**, *111*, 14423. (e) Maki, Y.; Ito, K.; Hosoya, N.; Yoneyama, C.; Furusawa, K.; Yamamoto, T.; Dobashi, T.; Sugimoto, Y.; Wakabayashi, K. *Biomacromolecules* **2011**, *12*, *2145*. (f) Furusawa, K. Sato, S.; Masumoto, J.; Hanazaki, Y.; Maki, Y.; Dobashi, T.; Yamamoto, T.; Fukui, A.; Sasaki, N. *Biomacromolecules* **2012**, *13*, 29.

(6) (a) Yang, W.; Furukawa, H.; Gong, J. P. *Adv. Mater.* **2008**, *20*, 4499. (b) Wu, Z. L.; Kurokawa, T.; Sawada, D.; Hu, J.; Furukawa, H.; Gong, J. P. *Macromolecules* **2011**, *44*, 3535.

(7) (a) Yokoyama, F.; Achife, C. E.; Matsuoka, M.; Shimamura, K.; Yamashita, Y.; Monobe, K. *Polymer* **1991**, *32*, 2911. (b) Yokoyama, F.; Achife, C. E.; Takahira, K.; Yamashita, Y.; Monobe, K.; Kusano, F.; Nishi, K. *J. Macromol. Sci. Phys.* **1992**, *B31*, 463.

(8) (a) Chrastil, J. *J. Agric. Food Chem.* **1991**, *39*, 874. (b) Mammarella, E. J.; Rubiolo, A. C. *Chem. Eng. J.* **2003**, *94*, 73. (c) Fall, A. B.; Lindström, S. B.; Sprakel, J.; Wågberg, L. *Soft Matter* **2013**, *9*, 1852. (d) Rokugawa, I.; Tomita, N.; Dobashi, T.; Yamamoto, T. *Soft Mater.* **2014**, *1*, 36.

(9) (a) Ziemecka, I.; Koper, G. J. M.; Olive, A. G. L.; van Esch, J. H. *Soft Matter* **2013**, *9*, 1556. (b) Morris, K. L.; Chen, L.; Raeburn, J.; Sellick, O. R.; Cotanda, P.; Paul, A.; Griffiths, P. C.; King, S. M.; O'Reilly, R. K.; Serpell, L. C.; Adams, D. J. *Nat. Commun.* **2013**, *4*, 1480. (c) Dobashi, T.; Tomita, N.; Maki, Y.; Chang, C. P.; Tamamoto, T. *Carbohyd. Polym.* **2011**, *84*, 709. (d) Montembault, A.; Viton, C.; Domard, A. *Biomacromolecules* **2005**, *6*, 653.

(10) Vandenberg, E. J.; Diveley, W. R.; Filar, L. J.; Pater, S. R.; Barth, H. G. *J. Polym. Sci, Part A: Polym. Chem.* **1989**, *27*, 3745.

(11) (a) Yang, W.; Furukawa, H.; Shigekura, Y.; Shikinaka, K.; Osada, Y.; Gong, J. P. *Macromolecules* **2008**, *41*, 1791. (b) Wu, Z. L.; Kurokawa, T.; Liang, S. M.; Gong, J. P. *Macromolecules* **2010**, *43*, 8202.

(12) (a) Wu, Z. L.; Arifuzzaman, M.; Kurokawa, T.; Le, K.; Hu, J.; Sun, T. L.; Furukawa, H.; Masunaga, H.; Gong, J. P. *Macromolecules* **2013**, *46*, 3581. (b) Wu, Z. L.; Kurokawa, T.; Liang, S. M.; Furukawa, H.; Gong, J. P. *J. Am. Chem. Soc.* **2010**, *132*, 10064.

(13) The gelation front is easy to be recognized by POM observation. Furthermore, at this region the appearance of the sample changed from transparent to turbid.

(14) Braschler, T.; Valero, A.; Colella, L.; Pataky, K.; Brugger, J.; Renaud, P. *Anal. Chem.* **2011**, *83*, 2234.

(15) The diffusion time, t, can be extend to ~20 min; within this period, good diffusion profile (e.g. linear relation of d^2 vs. t) can be obtained. When t > 40 min, PBDT solution became solid due to the severe solvent evaporation, which also led to increase in C_{Ca2+}.

(16) Einstein, A. *Investigations on the Theory of Bromnian Movement*, Dover: New York, **1926**.

(17) Lide, D. R. *Handbook of Chemistry and Physics*, 76th ed., CRC Press: Boca Raton, FL, **1995**.

(18) (a) Butler, J. C.; Angelini, T.; Tang, J. X.; Wong, G. C. L. *Phys. Rev. Lett.* **2003**, *91*, 028301. (b) Hsiao, P.-Y.; Luijten, E. *Phys. Rev. Lett.* **2006**, *97*, 148301.

(19) Unpublished data. A polyacrylamide (PAAm) gel containing randomly dispersed PBDT was synthesized and immersed in a $CaCl_2$ solution, in which PBDTs formed complex with Ca^{2+}. This hydrogel is optically isotropic, yet it shows strong birefringence under a small elongation strain, ε ~5%, indicating PBDT/Ca^{2+} complexes are easy to orient along the elongation direction. Without the formation of complex, the birefringence is not so sensitive to strain, as revealed in our previous work (Wu, Z. L.; Sawada, D.; Kurokawa, T.; Kakugo, A.; Yang, W.; Furukawa, H.; Gong, J. P. *Macromolecules* **2011**, *44*, 3542). Similar result was found in Curdlan gel (Maki, M.; Furusawa, K.; Yasuraoka, S.; Okamura, H.; Hosoya, N.; Sunaga, M.; Dobashi, T.; Sugimoto, Y.; Wakabayashi, K. *Carbohyd. Polym.* **2014**, *108*, 118).

(20) (a) Arifuzzaman, M.; Wu, Z. L.; Kurokawa, T.; Kakugo, A.; Gong, J. P. *Soft Matter* **2012**, *8*, 8060. (b) Arifuzzaman, M.; Wu, Z. L.; Takahashi, R.; Kurokawa, T.; Nakajima, T.; Gong, J. P. *Macromolecules* **2013**, *46*, 9083. (c) Takahashi, R.; Wu, Z. L.; Arifuzzaman, M.; Nonoyama, T.; Nakajima, T.; Kurokawa, T.; Gong, J. P. *Nat. Commun.* **2014**, *5*, 4490.

(21) (a) Hench, L. L.; West, J. K. *Chem. Rev.* **1990**, *90*, 33. (b) Chrastil, J. *J. Agric. Food Chem.* **1991**, *39*, 874. (c) Rehm, B. H. A. *Alginates: Biology and Applications*; Springer: Berlin, **2009**. (d) Donati, I.; Holtan, S.; Mørch, Y. A.; Borgogna, M.; Dentini, M.; Skjåk-Bræk, G. *Biomacromolecules* **2005**, *6*, 1031.

Table of contents

In situ observation of Ca^{2+} diffusion induced superstructure formation of a rigid polyanion

*Zi Liang Wu, Riku Takahashi, Daisuke Sawada, Md. Arifuzzaman, Tasuku Nakajima, Takayuki Kurokawa, Jian Hu, and Jian Ping Gong**